www.sciencemag.org/content/360/6384/aao7298/suppl/DC1

# Supplementary Materials for

## Structure of the herpes simplex virus 1 capsid with associated tegument protein complexes

Xinghong Dai and Z. Hong Zhou*

*Corresponding author. Email: hong.zhou@ucla.edu

Published 6 April 2018, *Science* **360**, eaao7298 (2018)
DOI: 10.1126/science.aao7298

**This PDF file includes:**

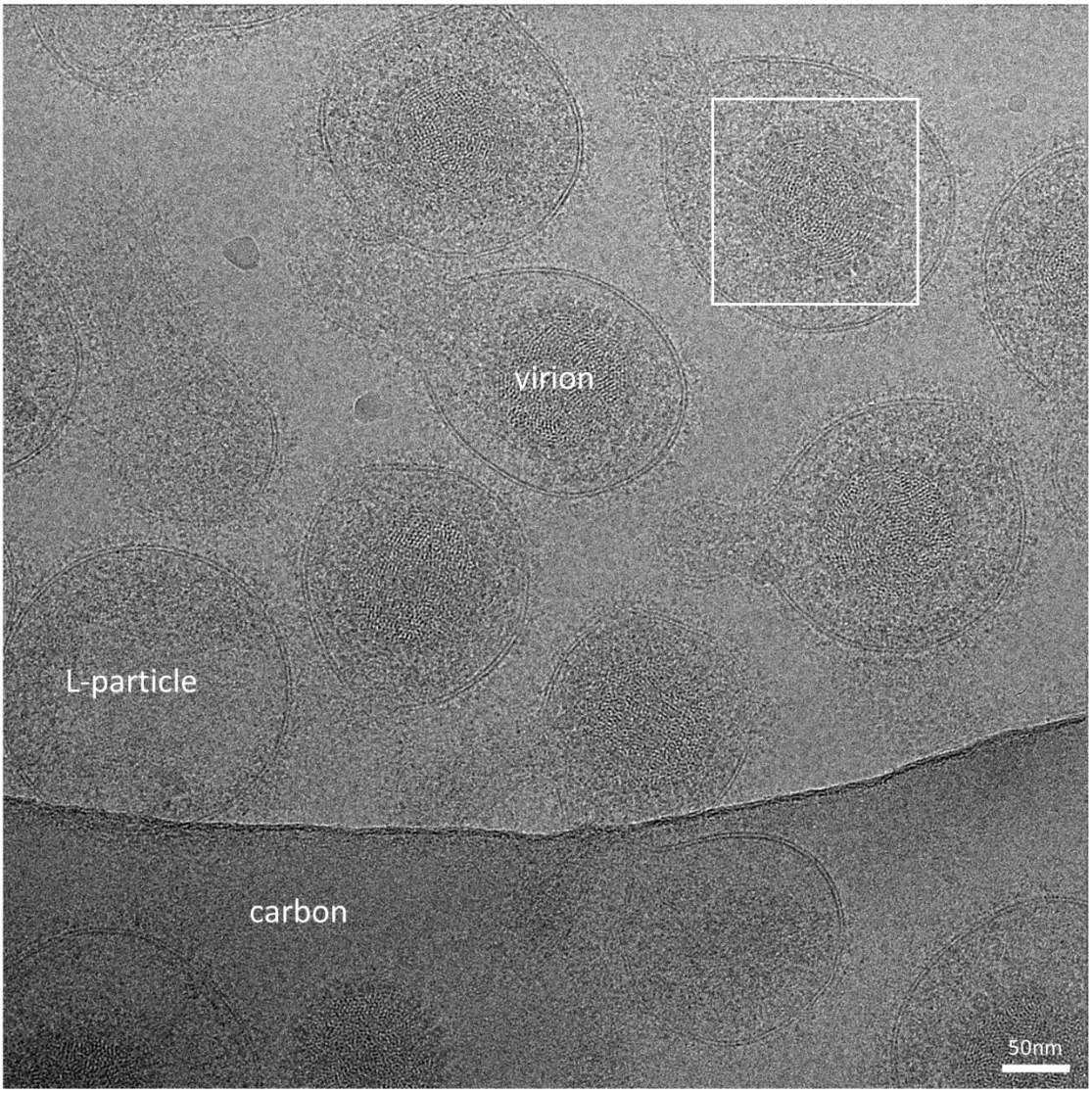


**Fig. S1. A cryoEM micrograph of HSV-1 virion.**

Good contrast of the image under relatively small defocus (-1.56 μm) indicates thin ice on the cryoEM grid. Also note that most particles are intact virions, a condition deliberately selected to preserve the CATC. L-particles ("light particles") are known to be noninfectious, enveloped viral particles containing tegument proteins but lacking nucleocapsid (*76*). The white box denotes the size of a particle image (1,440x1,440 pixels) boxed out from the micrograph for data processing. The box was roughly centered on the capsid.

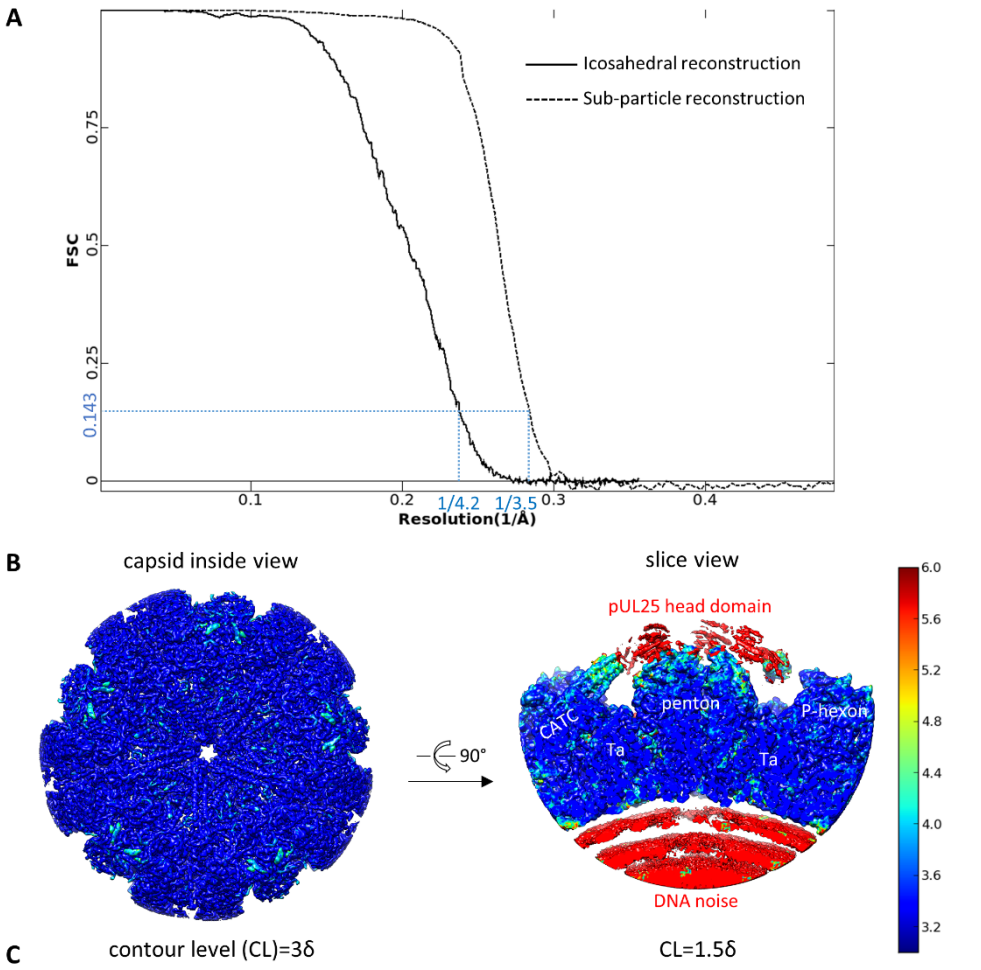


| Model refinement statistics | | | | | | | | | |
|---|---|---|---|---|---|---|---|---|---|
| Components | Model to map fit (CC around atoms) | R.m.s. deviations | | Validation | | | Ramachandran plot | | |
| | | Bond lengths (Å) | Bond angels (°) | Clashscore | MolProbity score | Poor rotamers (%) | Favored (%) | Allowed (%) | Outlier (%) |
| MCP (P2) | 0.83 | 0.006 | 0.85 | 4.04 | 1.59 | 0.19 | 93.92 | 6.08 | 0.00 |
| SCP (P2) | 0.81 | 0.005 | 0.76 | 1.31 | 0.86 | 0.00 | 98.99 | 1.01 | 0.00 |
| Triplex (Ta) | 0.83 | 0.006 | 0.93 | 3.59 | 1.50 | 0.78 | 94.87 | 4.91 | 0.22 |
| Tegument | 0.82 | 0.007 | 0.86 | 3.05 | 1.37 | 0.00 | 95.97 | 4.03 | 0.00 |

**Fig. S2. Resolution and model quality assessment.**

(**A**) Gold-standard Fourier shell correlation (FSC) curves of the cryoEM reconstructions. Resolution of the icosahedral reconstruction by treating the capsid as a whole was 4.2 Å, and resolution of the sub-particle reconstruction of the vertex region was 3.5 Å, based on the FSC = 0.143 criterion (*68*). (**B**) Resmap (*77*) assessment of local resolution in the sub-particle reconstruction map of the vertex region. Note that majority of the CATC density reaches 3.5 Å resolution or even better, except distal region of the five-helix bundle (~4 Å) and the pUL25 head domain (~6 Å). A relatively low contour level (1.5δ, δ is the standard deviation) was chosen for the right panel to show densities of the flexible pUL25 head domain. (**C**) Model statistics reported by Phenix real space refinement (*71*).

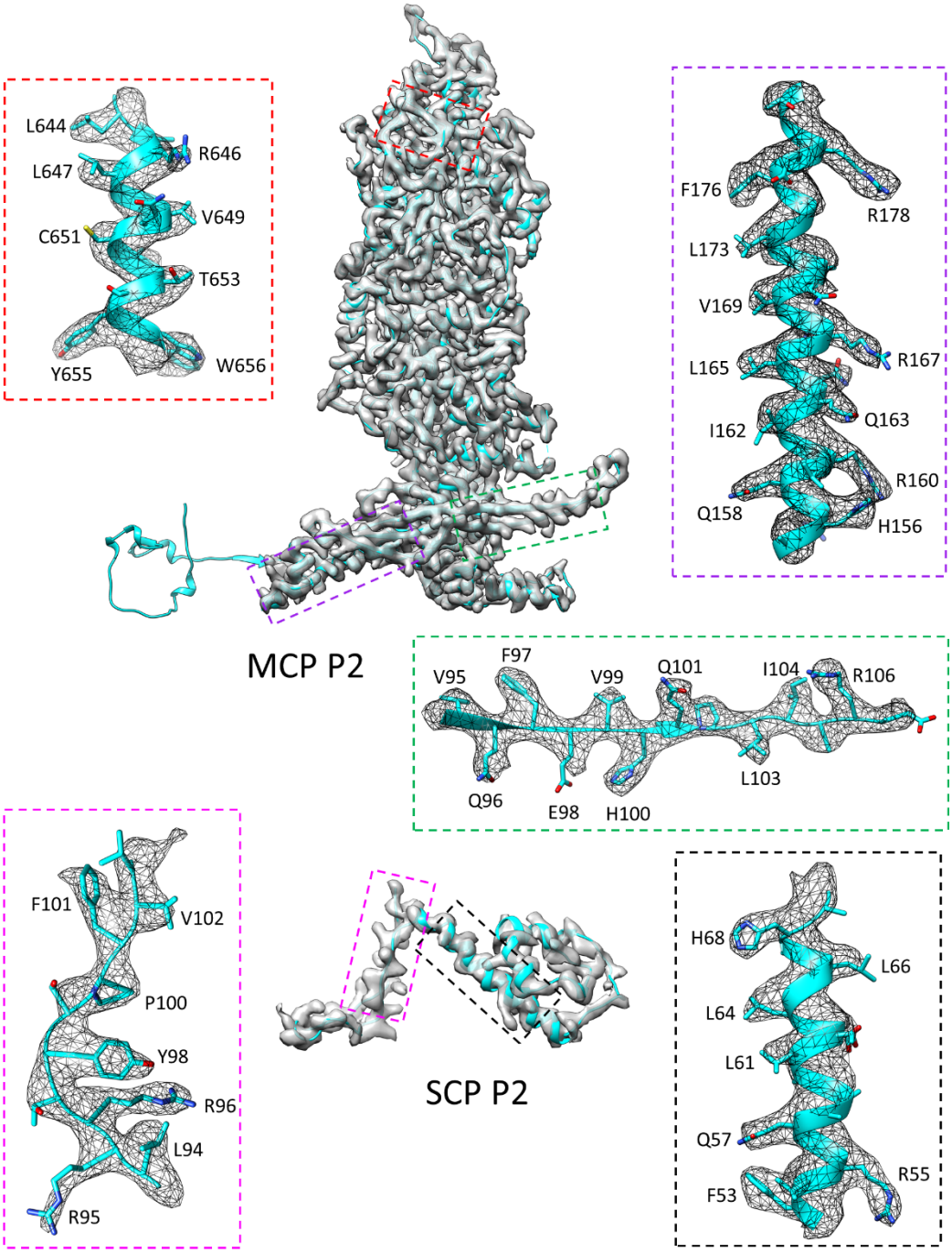


**Fig. S3. Density maps and atomic models of MCP and SCP.**

Densities of MCP P2 and SCP P2 (see Fig. 1C for nomenclature) were segmented out from the 3.5 Å resolution sub-particle reconstruction map of the vertex region. The boxed regions were zoomed-in to illustrate residue features in the density map. Note that the N-lasso region of MCP P2 has extended out of the sub-particle reconstruction area, so its density is not shown here.

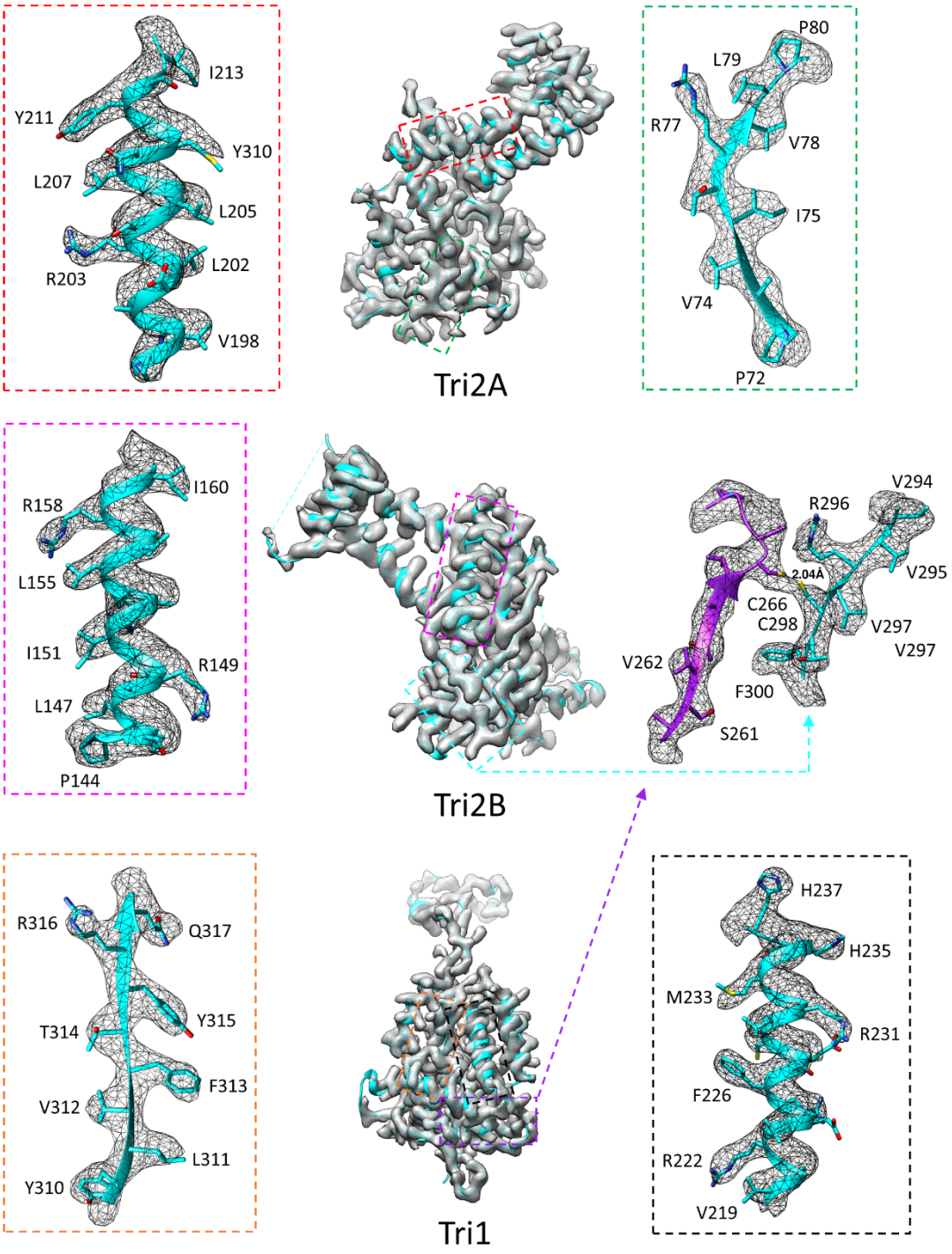


**Fig. S4. Density maps and atomic models of Tri1, Tri2A and Tri2B.**

Densities of triplex Ta components were segmented out from the 3.5 Å resolution sub-particle reconstruction map of the vertex region. The boxed regions were zoomed-in to illustrate residue features in the density map. The middle right panel shows density connection between Tri1 Cys266 and Tri2B Cys298, indicating an inter-molecular disulfide bond.

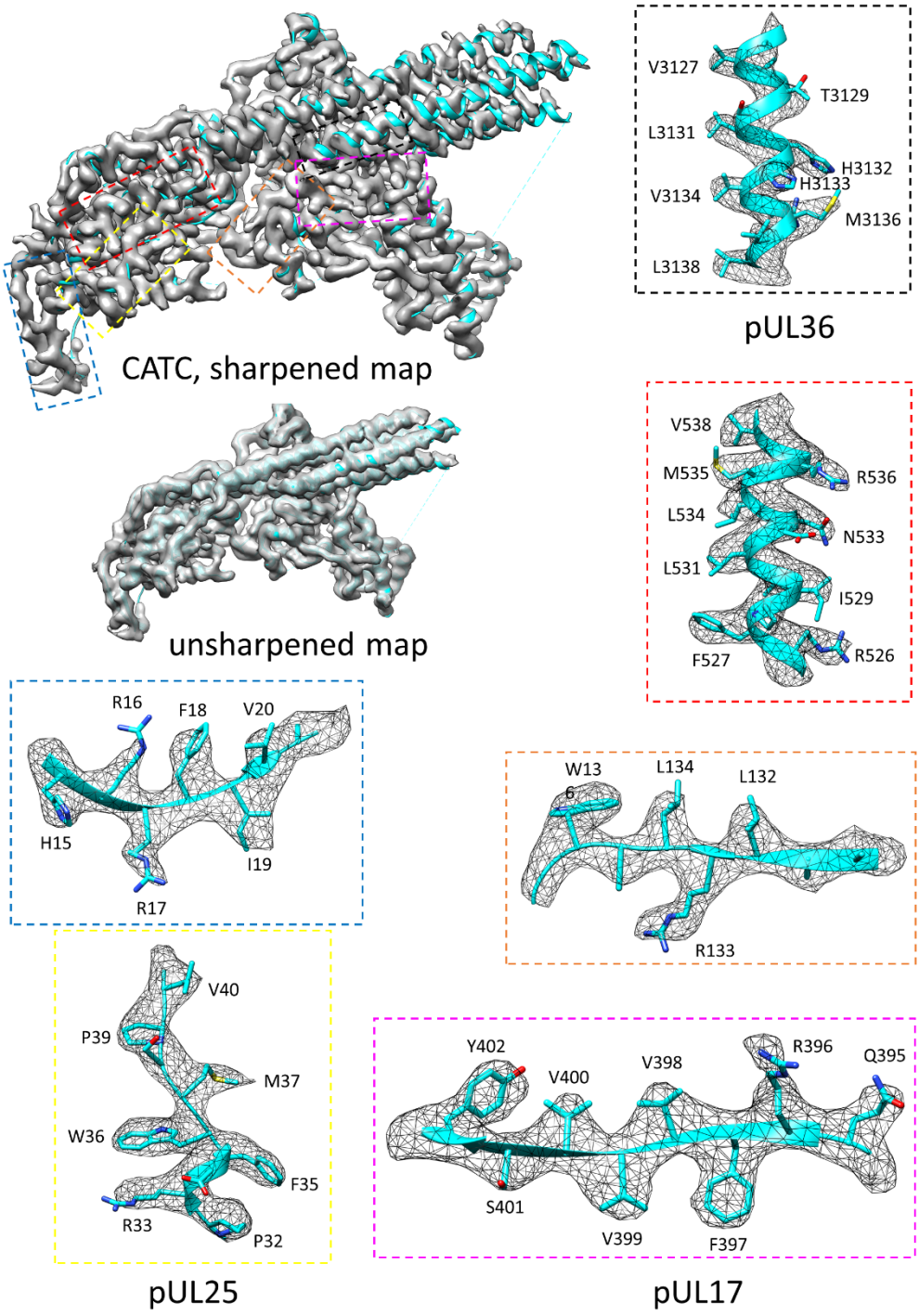


**Fig. S5. Density map and atomic model of the CATC.**

Densities of the CATC were segmented out from the 3.5 Å resolution sub-particle reconstruction map of the vertex region. The boxed regions were zoomed-in to illustrate residue features in the density map. An unsharpened map of the CATC is also shown to illustrate well-resolved helices in the capsid-distal region of the five-helix bundle, which is broken and noisy in the sharpened map due to higher flexibility.

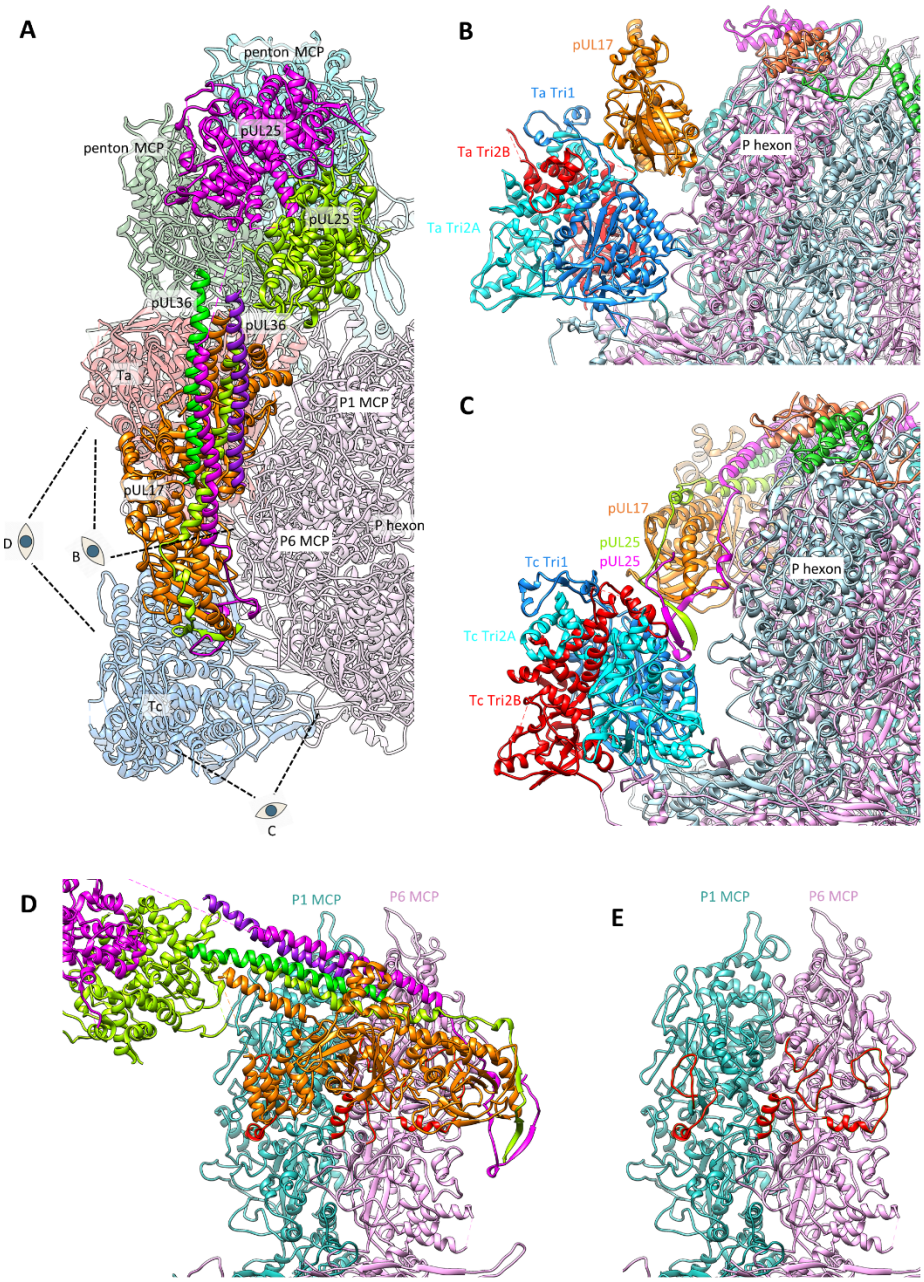


**Fig. S6. P-hexon provides support for CATC binding to triplex pair Ta/Tc.**

(**A**) Structure of CATC and its interacting capsid components viewed from outside of the capsid. This figure is a zoom-in view of Figure 2D. It serves as a roadmap to denote the positions of viewpoint (eye marks) for panels (B) to (D). (**B** and **C**) P-hexon provides support for CATC binding to triplexes Ta (B) and Tc (C). In both cases, the CATC sits on the shoulder of the triplex, and leans against the out surface of the P-hexon tower on the other side. For clarity, only part of the pUL17 model is shown in panel (B). (**D**) Relative position of the CATC to the supporting P1 and P6 MCPs. (**E**) P1 and P6 MCP surface segments (red colored) directly involved in contact with pUL17 of the CATC.

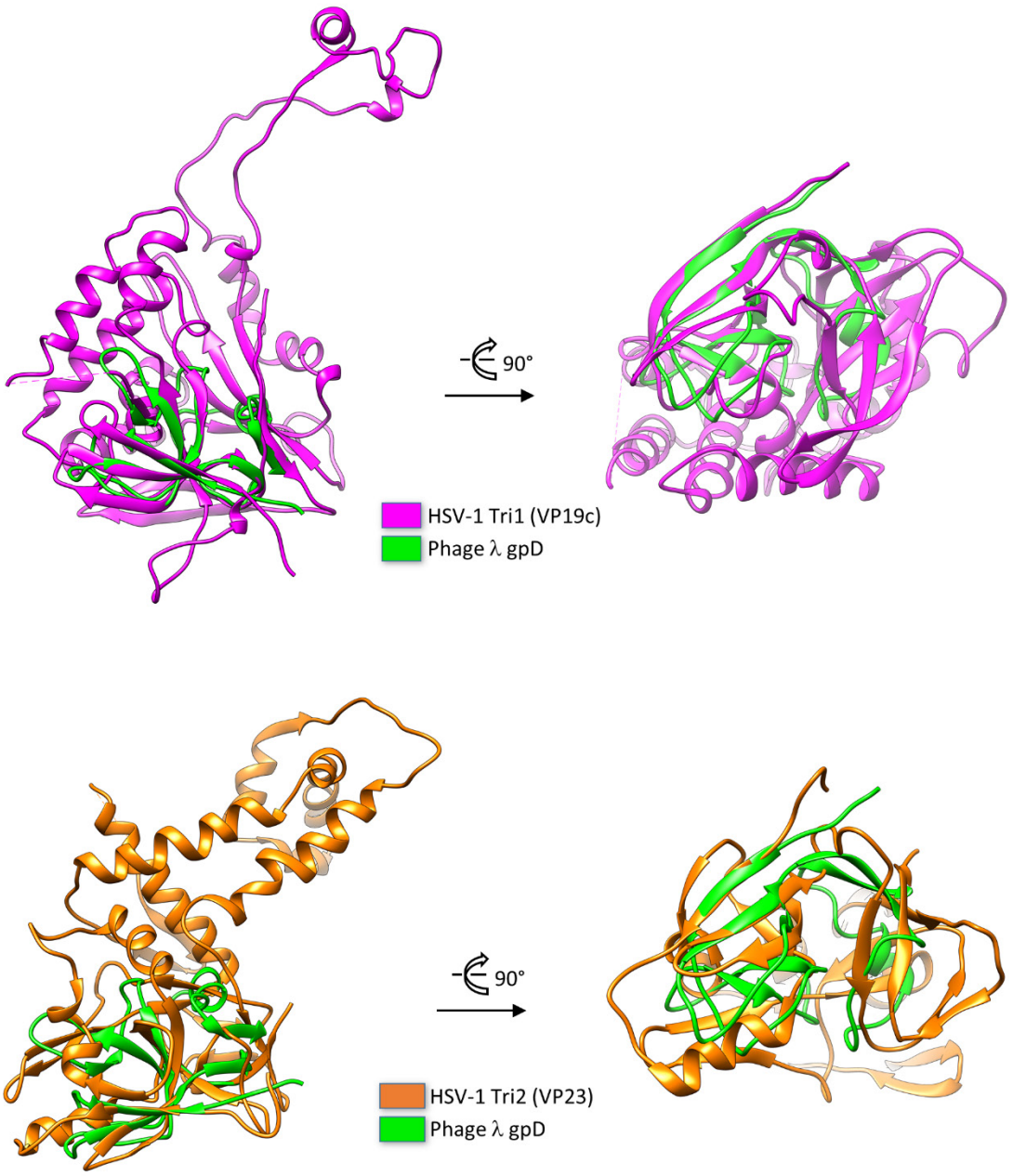


**Fig. S7. Structural alignments between bacteriophage λ gpD and HSV-1 Tri1 (VP19c) or Tri2 (VP23).**

Fold similarities among the three are indicative of close evolutionary relationship.

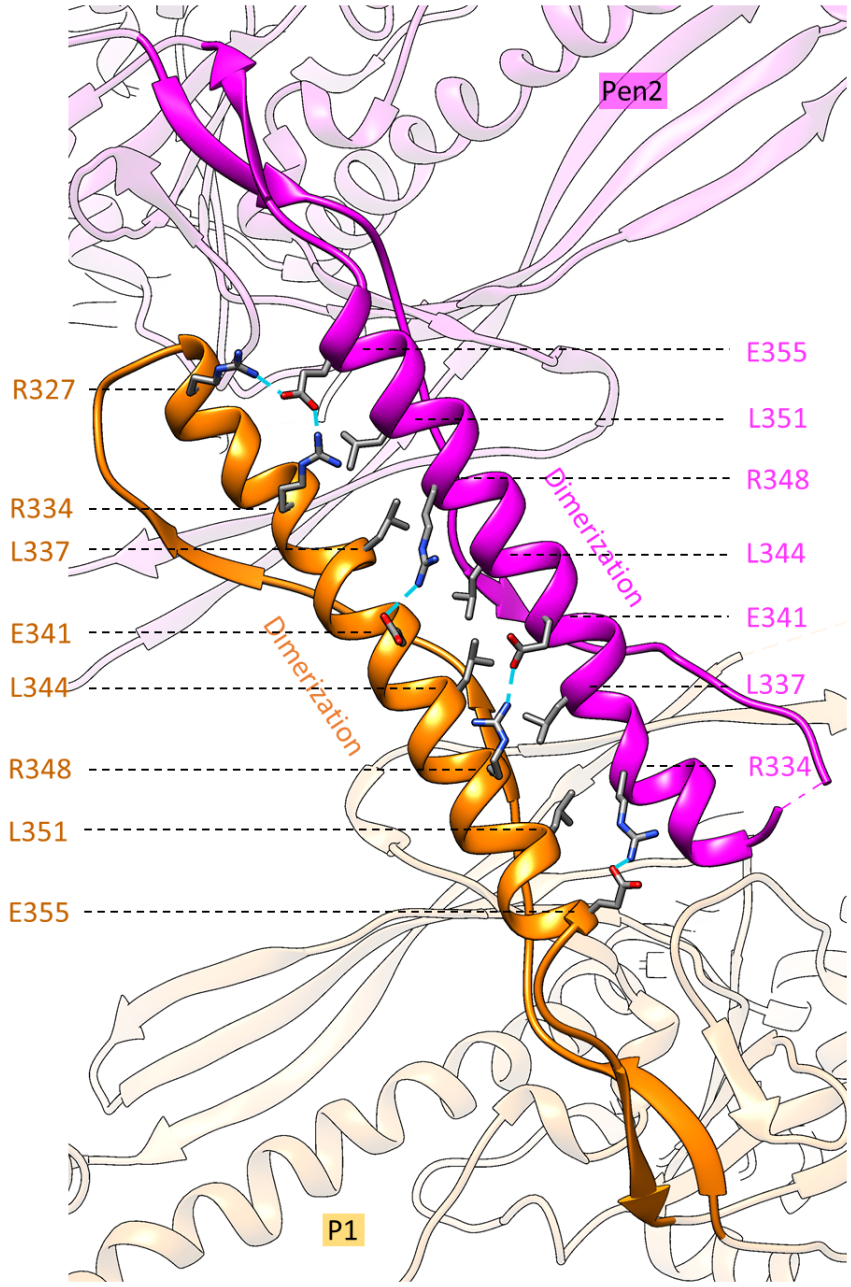


**Fig. S8. Interactions between the refolded dimerization domains of a penton MCP and a P1 hexon MCP.**

The dimerization domains of penton MCP and P1 hexon MCP both refold from the canonical helix-turn-helix structure (*cf.* Fig. 4I) into a single, long helix. The two resulting helices are paired together via hydrophobic interactions of buried, interdigitated leucine residues, as well as multiple hydrogen bonds between arginine and glutamate residues exposed on the inner surface of the capsid.

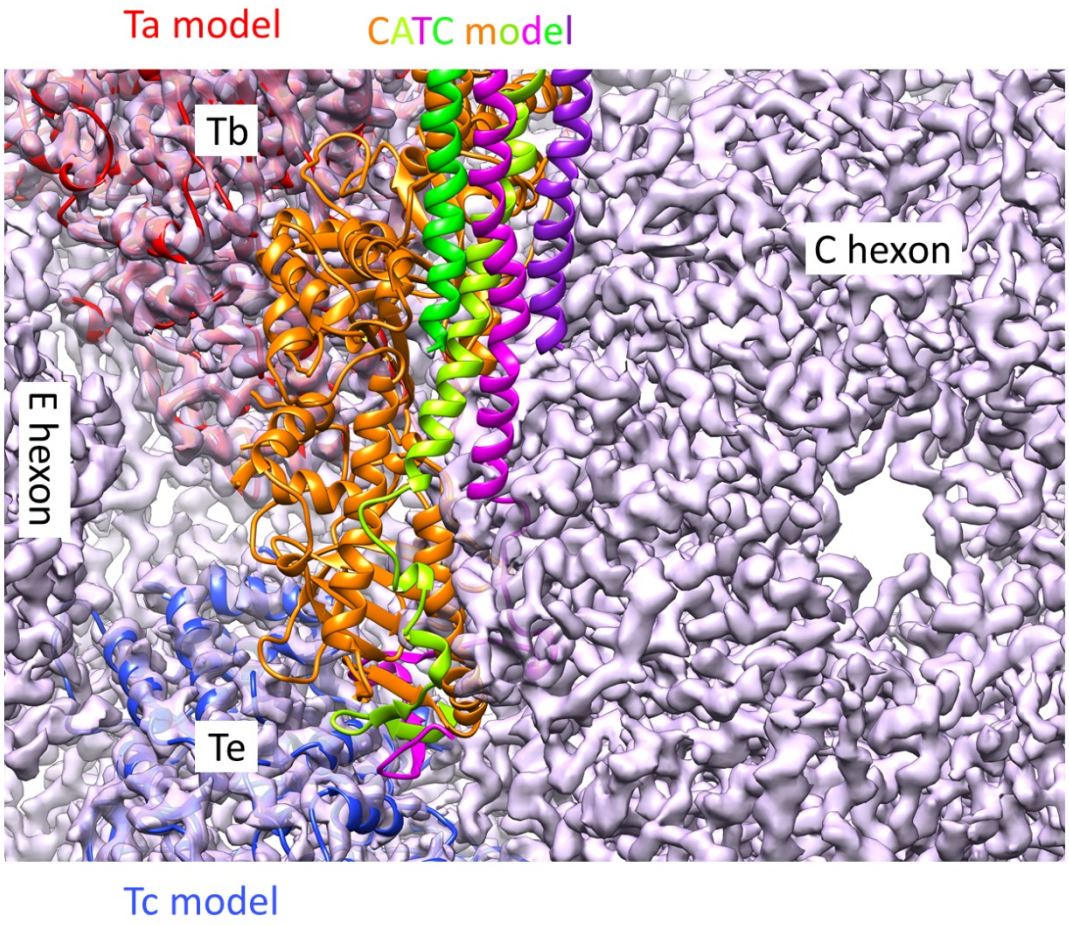


**Fig. S9. Steric hindrance of C-hexon prevents CATC from binding to triplex pair Tb/Te.**
Atomic models of triplexes Ta (red), Tc (blue) and the bound CATC (gold to purple) are fitted as a rigid unit into the cryoEM density map (semitransparent pink surface) of triplexes Tb, Te in between an E-hexon and a C-hexon. The agreement between Ta/Tc models and Tb/Te densities suggests that triplex pair Tb/Te bears the same geometry as triplex pair Ta/Tc, and thus would also be able to support CATC binding. However, crushing of the CATC model into the C-hexon density suggests that the C-hexon presents a steric hindrance which would prevent the CATC from binding to triplex pair Tb/Te.

**References**


1. P. Pellett, B. Roizman, in *Fields Virology*, D. Knipe, P. Howley, Eds. (Lippincott Williams and Wilkins, Philadelphia, 2013), vol. 2, pp. 1802–1822.

2. G. A. Smith, L. W. Enquist, Break ins and break outs: Viral interactions with the cytoskeleton of mammalian cells. *Annu. Rev. Cell Dev. Biol.* **18**, 135–161 (2002). doi:10.1146/annurev.cellbio.18.012502.105920 Medline

3. G. W. Luxton, S. Haverlock, K. E. Coller, S. E. Antinone, A. Pincetic, G. A. Smith, Targeting of herpesvirus capsid transport in axons is coupled to association with specific sets of tegument proteins. *Proc. Natl. Acad. Sci. U.S.A.* **102**, 5832–5837 (2005). doi:10.1073/pnas.0500803102 Medline

4. G. W. Luxton, J. I. Lee, S. Haverlock-Moyns, J. M. Schober, G. A. Smith, The pseudorabies virus VP1/2 tegument protein is required for intracellular capsid transport. *J. Virol.* **80**, 201–209 (2006). doi:10.1128/JVI.80.1.201-209.2006 Medline

5. S. E. Antinone, G. A. Smith, Retrograde axon transport of herpes simplex virus and pseudorabies virus: A live-cell comparative analysis. *J. Virol.* **84**, 1504–1512 (2010). doi:10.1128/JVI.02029-09 Medline

6. S. V. Zaichick, K. P. Bohannon, G. A. Smith, Alphaherpesviruses and the cytoskeleton in neuronal infections. *Viruses* **3**, 941–981 (2011). doi:10.3390/v3070941 Medline

7. S. V. Zaichick, K. P. Bohannon, A. Hughes, P. J. Sollars, G. E. Pickard, G. A. Smith, The herpesvirus VP1/2 protein is an effector of dynein-mediated capsid transport and neuroinvasion. *Cell Host Microbe* **13**, 193–203 (2013). doi:10.1016/j.chom.2013.01.009 Medline

8. Z. H. Zhou, D. H. Chen, J. Jakana, F. J. Rixon, W. Chiu, Visualization of tegument-capsid interactions and DNA in intact herpes simplex virus type 1 virions. *J. Virol.* **73**, 3210–3218 (1999). Medline

9. B. L. Trus, W. W. Newcomb, N. Cheng, G. Cardone, L. Marekov, F. L. Homa, J. C. Brown, A. C. Steven, Allosteric signaling and a nuclear exit strategy: Binding of UL25/UL17 heterodimers to DNA-filled HSV-1 capsids. *Mol. Cell* **26**, 479–489 (2007). doi:10.1016/j.molcel.2007.04.010 Medline

10. K. Toropova, J. B. Huffman, F. L. Homa, J. F. Conway, The herpes simplex virus 1 UL17 protein is the second constituent of the capsid vertex-specific component required for DNA packaging and retention. *J. Virol.* **85**, 7513–7522 (2011). doi:10.1128/JVI.00837-11 Medline

11. X. Dai, D. Gong, T. T. Wu, R. Sun, Z. H. Zhou, Organization of capsid-associated tegument components in Kaposi's sarcoma-associated herpesvirus. *J. Virol.* **88**, 12694–12702 (2014). doi:10.1128/JVI.01509-14 Medline

12. J. F. Conway, S. K. Cockrell, A. M. Copeland, W. W. Newcomb, J. C. Brown, F. L. Homa, Labeling and localization of the herpes simplex virus capsid protein UL25 and its interaction with the two triplexes closest to the penton. *J. Mol. Biol.* **397**, 575–586 (2010). doi:10.1016/j.jmb.2010.01.043 Medline

13. S. K. Cockrell, J. B. Huffman, K. Toropova, J. F. Conway, F. L. Homa, Residues of the UL25 protein of herpes simplex virus that are required for its stable interaction with capsids. *J. Virol.* **85**, 4875–4887 (2011). doi:10.1128/JVI.00242-11 Medline

14. F. L. Homa, J. B. Huffman, K. Toropova, H. R. Lopez, A. M. Makhov, J. F. Conway, Structure of the pseudorabies virus capsid: Comparison with herpes simplex virus type 1 and differential binding of essential minor proteins. *J. Mol. Biol.* **425**, 3415–3428 (2013). doi:10.1016/j.jmb.2013.06.034 Medline

15. G. Cardone, W. W. Newcomb, N. Cheng, P. T. Wingfield, B. L. Trus, J. C. Brown, A. C. Steven, The UL36 tegument protein of herpes simplex virus 1 has a composite binding site at the capsid vertices. *J. Virol.* **86**, 4058–4064 (2012). doi:10.1128/JVI.00012-12 Medline

16. W. H. Fan, A. P. Roberts, M. McElwee, D. Bhella, F. J. Rixon, R. Lauder, The large tegument protein pUL36 is essential for formation of the capsid vertex-specific component at the capsid-tegument interface of herpes simplex virus 1. *J. Virol.* **89**, 1502–1511 (2015). doi:10.1128/JVI.02887-14 Medline

17. A. Huet, A. M. Makhov, J. B. Huffman, M. Vos, F. L. Homa, J. F. Conway, Extensive subunit contacts underpin herpesvirus capsid stability and interior-to-exterior allostery. *Nat. Struct. Mol. Biol.* **23**, 531–539 (2016). doi:10.1038/nsmb.3212 Medline

18. X. Yu, S. Shah, M. Lee, W. Dai, P. Lo, W. Britt, H. Zhu, F. Liu, Z. H. Zhou, Biochemical and structural characterization of the capsid-bound tegument proteins of human cytomegalovirus. *J. Struct. Biol.* **174**, 451–460 (2011). doi:10.1016/j.jsb.2011.03.006 Medline

19. X. Dai, X. Yu, H. Gong, X. Jiang, G. Abenes, H. Liu, S. Shivakoti, W. J. Britt, H. Zhu, F. Liu, Z. H. Zhou, The smallest capsid protein mediates binding of the essential tegument protein pp150 to stabilize DNA-containing capsids in human cytomegalovirus. *PLOS Pathog.* **9**, e1003525 (2013). doi:10.1371/journal.ppat.1003525 Medline

20. X. Yu, J. Jih, J. Jiang, Z. H. Zhou, Atomic structure of the human cytomegalovirus capsid with its securing tegument layer of pp150. *Science* **356**, eaam6892 (2017). doi:10.1126/science.aam6892 Medline

21. Z. H. Zhou, M. Dougherty, J. Jakana, J. He, F. J. Rixon, W. Chiu, Seeing the herpesvirus capsid at 8.5 Å. *Science* **288**, 877–880 (2000). doi:10.1126/science.288.5467.877 Medline

22. B. R. Bowman, R. L. Welschhans, H. Jayaram, N. D. Stow, V. G. Preston, F. A. Quiocho, Structural characterization of the UL25 DNA-packaging protein from herpes simplex virus type 1. *J. Virol.* **80**, 2309–2317 (2006). doi:10.1128/JVI.80.5.2309-2317.2006 Medline

23. J. I. Lee, G. W. Luxton, G. A. Smith, Identification of an essential domain in the herpesvirus VP1/2 tegument protein: The carboxy terminus directs incorporation into capsid assemblons. *J. Virol.* **80**, 12086–12094 (2006). doi:10.1128/JVI.01184-06 Medline

24. K. E. Coller, J. I. Lee, A. Ueda, G. A. Smith, The capsid and tegument of the alphaherpesviruses are linked by an interaction between the UL25 and VP1/2 proteins. *J. Virol.* **81**, 11790–11797 (2007). doi:10.1128/JVI.01113-07 Medline

25. M. Leelawong, J. I. Lee, G. A. Smith, Nuclear egress of pseudorabies virus capsids is enhanced by a subspecies of the large tegument protein that is lost upon cytoplasmic maturation. *J. Virol.* **86**, 6303–6314 (2012). doi:10.1128/JVI.07051-11 Medline

26. F. Yang, P. Forrer, Z. Dauter, J. F. Conway, N. Cheng, M. E. Cerritelli, A. C. Steven, A. Plückthun, A. Wlodawer, Novel fold and capsid-binding properties of the λ-phage display platform protein gpD. *Nat. Struct. Biol.* **7**, 230–237 (2000). doi:10.1038/73347 Medline

27. G. C. Lander, A. Evilevitch, M. Jeembaeva, C. S. Potter, B. Carragher, J. E. Johnson, Bacteriophage lambda stabilization by auxiliary protein gpD: Timing, location, and mechanism

of attachment determined by cryo-EM. *Structure* **16**, 1399–1406 (2008). doi:10.1016/j.str.2008.05.016 Medline

28. X. Dai, D. Gong, H. Lim, J. Jih, T. T. Wu, R. Sun, Z. H. Zhou, Structure and mutagenesis reveal essential capsid protein interactions for KSHV replication. *Nature* **553**, 521–525 (2018). doi:10.1038/nature25438 Medline

29. X. Dai, D. Gong, Y. Xiao, T. T. Wu, R. Sun, Z. H. Zhou, CryoEM and mutagenesis reveal that the smallest capsid protein cements and stabilizes Kaposi's sarcoma-associated herpesvirus capsid. *Proc. Natl. Acad. Sci. U.S.A.* **112**, E649–E656 (2015). doi:10.1073/pnas.1420317112 Medline

30. P. Desai, N. A. DeLuca, S. Person, Herpes simplex virus type 1 VP26 is not essential for replication in cell culture but influences production of infectious virus in the nervous system of infected mice. *Virology* **247**, 115–124 (1998). doi:10.1006/viro.1998.9230 Medline

31. M. L. Baker, W. Jiang, F. J. Rixon, W. Chiu, Common ancestry of herpesviruses and tailed DNA bacteriophages. *J. Virol.* **79**, 14967–14970 (2005). doi:10.1128/JVI.79.23.14967-14970.2005 Medline

32. F. J. Rixon, M. F. Schmid, Structural similarities in DNA packaging and delivery apparatuses in herpesvirus and dsDNA bacteriophages. *Curr. Opin. Virol.* **5**, 105–110 (2014). doi:10.1016/j.coviro.2014.02.003 Medline

33. R. L. Duda, Protein chainmail: Catenated protein in viral capsids. *Cell* **94**, 55–60 (1998). doi:10.1016/S0092-8674(00)81221-0 Medline

34. W. R. Wikoff, L. Liljas, R. L. Duda, H. Tsuruta, R. W. Hendrix, J. E. Johnson, Topologically linked protein rings in the bacteriophage HK97 capsid. *Science* **289**, 2129–2133 (2000). doi:10.1126/science.289.5487.2129 Medline

35. A. A. Aksyuk, W. W. Newcomb, N. Cheng, D. C. Winkler, J. Fontana, J. B. Heymann, A. C. Steven, Subassemblies and asymmetry in assembly of herpes simplex virus procapsid. *mBio* **6**, e01525–e15 (2015). doi:10.1128/mBio.01525-15 Medline

36. J. V. Spencer, W. W. Newcomb, D. R. Thomsen, F. L. Homa, J. C. Brown, Assembly of the herpes simplex virus capsid: Preformed triplexes bind to the nascent capsid. *J. Virol.* **72**, 3944–3951 (1998). Medline

37. B. L. Trus, F. P. Booy, W. W. Newcomb, J. C. Brown, F. L. Homa, D. R. Thomsen, A. C. Steven, The herpes simplex virus procapsid: Structure, conformational changes upon maturation, and roles of the triplex proteins VP19c and VP23 in assembly. *J. Mol. Biol.* **263**, 447–462 (1996). doi:10.1016/S0022-2836(96)80018-0 Medline

38. J. Snijder, K. Radtke, F. Anderson, L. Scholtes, E. Corradini, J. Baines, A. J. R. Heck, G. J. L. Wuite, B. Sodeik, W. H. Roos, Vertex-specific proteins pUL17 and pUL25 mechanically reinforce herpes simplex virus capsids. *J. Virol.* **91**, e00123-17 (2017). doi:10.1128/JVI.00123-17 Medline

39. H. Granzow, B. G. Klupp, T. C. Mettenleiter, Entry of pseudorabies virus: An immunogold-labeling study. *J. Virol.* **79**, 3200–3205 (2005). doi:10.1128/JVI.79.5.3200-3205.2005 Medline

40. M. McElwee, F. Beilstein, M. Labetoulle, F. J. Rixon, D. Pasdeloup, Dystonin/BPAG1 promotes plus-end-directed transport of herpes simplex virus 1 capsids on microtubules during entry. *J. Virol.* **87**, 11008–11018 (2013). doi:10.1128/JVI.01633-13 Medline

41. V. G. Preston, J. Murray, C. M. Preston, I. M. McDougall, N. D. Stow, The UL25 gene product of herpes simplex virus type 1 is involved in uncoating of the viral genome. *J. Virol.* **82**, 6654–6666 (2008). doi:10.1128/JVI.00257-08 Medline

42. D. Pasdeloup, D. Blondel, A. L. Isidro, F. J. Rixon, Herpesvirus capsid association with the nuclear pore complex and viral DNA release involve the nucleoporin CAN/Nup214 and the capsid protein pUL25. *J. Virol.* **83**, 6610–6623 (2009). doi:10.1128/JVI.02655-08 Medline

43. J. B. Huffman, G. R. Daniel, E. Falck-Pedersen, A. Huet, G. A. Smith, J. F. Conway, F. L. Homa, The C terminus of the herpes simplex virus UL25 protein is required for release of viral genomes from capsids bound to nuclear pores. *J. Virol.* **91**, e00641-17 (2017). doi:10.1128/JVI.00641-17 Medline

44. B. G. Klupp, H. Granzow, G. M. Keil, T. C. Mettenleiter, The capsid-associated UL25 protein of the alphaherpesvirus pseudorabies virus is nonessential for cleavage and encapsidation of genomic DNA but is required for nuclear egress of capsids. *J. Virol.* **80**, 6235–6246 (2006). doi:10.1128/JVI.02662-05 Medline

45. K. Yang, J. D. Baines, Selection of HSV capsids for envelopment involves interaction between capsid surface components pUL31, pUL17, and pUL25. *Proc. Natl. Acad. Sci. U.S.A.* **108**, 14276–14281 (2011). doi:10.1073/pnas.1108564108 Medline

46. M. Leelawong, D. Guo, G. A. Smith, A physical link between the pseudorabies virus capsid and the nuclear egress complex. *J. Virol.* **85**, 11675–11684 (2011). doi:10.1128/JVI.05614-11 Medline

47. T. C. Mettenleiter, F. Müller, H. Granzow, B. G. Klupp, The way out: What we know and do not know about herpesvirus nuclear egress. *Cell. Microbiol.* **15**, 170–178 (2013). doi:10.1111/cmi.12044 Medline

48. W. W. Newcomb, J. Fontana, D. C. Winkler, N. Cheng, J. B. Heymann, A. C. Steven, The primary enveloped virion of herpes simplex virus 1: Its role in nuclear egress. *mBio* **8**, e00825-17 (2017). doi:10.1128/mBio.00825-17 Medline

49. P. J. Desai, A null mutation in the UL36 gene of herpes simplex virus type 1 results in accumulation of unenveloped DNA-filled capsids in the cytoplasm of infected cells. *J. Virol.* **74**, 11608–11618 (2000). doi:10.1128/JVI.74.24.11608-11618.2000 Medline

50. B. G. Klupp, W. Fuchs, H. Granzow, R. Nixdorf, T. C. Mettenleiter, Pseudorabies virus UL36 tegument protein physically interacts with the UL37 protein. *J. Virol.* **76**, 3065–3071 (2002). doi:10.1128/JVI.76.6.3065-3071.2002 Medline

51. B. Mijatov, A. L. Cunningham, R. J. Diefenbach, Residues F593 and E596 of HSV-1 tegument protein pUL36 (VP1/2) mediate binding of tegument protein pUL37. *Virology* **368**, 26–31 (2007). doi:10.1016/j.virol.2007.07.005 Medline

52. D. H. Ko, A. L. Cunningham, R. J. Diefenbach, The major determinant for addition of tegument protein pUL48 (VP16) to capsids in herpes simplex virus type 1 is the presence of the major tegument protein pUL36 (VP1/2). *J. Virol.* **84**, 1397–1405 (2010). doi:10.1128/JVI.01721-09 Medline

53. Q. Zhu, R. J. Courtney, Chemical cross-linking of virion envelope and tegument proteins of herpes simplex virus type 1. *Virology* **204**, 590–599 (1994). doi:10.1006/viro.1994.1573 Medline

54. S. T. Gross, C. A. Harley, D. W. Wilson, The cytoplasmic tail of herpes simplex virus glycoprotein H binds to the tegument protein VP16 in vitro and in vivo. *Virology* **317**, 1–12 (2003). doi:10.1016/j.virol.2003.08.023 Medline

55. D. E. Kamen, S. T. Gross, M. E. Girvin, D. W. Wilson, Structural basis for the physiological temperature dependence of the association of VP16 with the cytoplasmic tail of herpes simplex virus glycoprotein H. *J. Virol.* **79**, 6134–6141 (2005). doi:10.1128/JVI.79.10.6134-6141.2005 Medline

56. N. Jambunathan, D. Chouljenko, P. Desai, A. S. Charles, R. Subramanian, V. N. Chouljenko, K. G. Kousoulas, Herpes simplex virus 1 protein UL37 interacts with viral glycoprotein gK and membrane protein UL20 and functions in cytoplasmic virion envelopment. *J. Virol.* **88**, 5927–5935 (2014). doi:10.1128/JVI.00278-14 Medline

57. N. Scrima, J. Lepault, Y. Boulard, D. Pasdeloup, S. Bressanelli, S. Roche, Insights into herpesvirus tegument organization from structural analyses of the 970 central residues of HSV-1 UL36 protein. *J. Biol. Chem.* **290**, 8820–8833 (2015). doi:10.1074/jbc.M114.612838 Medline

58. G. Woehlke, M. Schliwa, Walking on two heads: The many talents of kinesin. *Nat. Rev. Mol. Cell Biol.* **1**, 50–58 (2000). doi:10.1038/35036069 Medline

59. N. Hirokawa, K. K. Pfister, H. Yorifuji, M. C. Wagner, S. T. Brady, G. S. Bloom, Submolecular domains of bovine brain kinesin identified by electron microscopy and monoclonal antibody decoration. *Cell* **56**, 867–878 (1989). doi:10.1016/0092-8674(89)90691-0 Medline

60. F. J. Kull, E. P. Sablin, R. Lau, R. J. Fletterick, R. D. Vale, Crystal structure of the kinesin motor domain reveals a structural similarity to myosin. *Nature* **380**, 550–555 (1996). doi:10.1038/380550a0 Medline

61. C. Suloway, J. Pulokas, D. Fellmann, A. Cheng, F. Guerra, J. Quispe, S. Stagg, C. S. Potter, B. Carragher, Automated molecular microscopy: The new Leginon system. *J. Struct. Biol.* **151**, 41–60 (2005). doi:10.1016/j.jsb.2005.03.010 Medline

62. X. Li, P. Mooney, S. Zheng, C. R. Booth, M. B. Braunfeld, S. Gubbens, D. A. Agard, Y. Cheng, Electron counting and beam-induced motion correction enable near-atomic-resolution single-particle cryo-EM. *Nat. Methods* **10**, 584–590 (2013). doi:10.1038/nmeth.2472 Medline

63. J. A. Mindell, N. Grigorieff, Accurate determination of local defocus and specimen tilt in electron microscopy. *J. Struct. Biol.* **142**, 334–347 (2003). doi:10.1016/S1047-8477(03)00069-8 Medline

64. S. J. Ludtke, P. R. Baldwin, W. Chiu, EMAN: Semiautomated software for high-resolution single-particle reconstructions. *J. Struct. Biol.* **128**, 82–97 (1999). doi:10.1006/jsbi.1999.4174 Medline

65. Y. Liang, E. Y. Ke, Z. H. Zhou, IMIRS: A high-resolution 3D reconstruction package integrated with a relational image database. *J. Struct. Biol.* **137**, 292–304 (2002). doi:10.1016/S1047-8477(02)00014-X Medline

66. H. Liu, L. Cheng, S. Zeng, C. Cai, Z. H. Zhou, Q. Yang, Symmetry-adapted spherical harmonics method for high-resolution 3D single-particle reconstructions. *J. Struct. Biol.* **161**, 64–73 (2008). doi:10.1016/j.jsb.2007.09.016 Medline

67. X. Zhang, X. Zhang, Z. H. Zhou, Low cost, high performance GPU computing solution for atomic resolution cryoEM single-particle reconstruction. *J. Struct. Biol.* **172**, 400–406 (2010). doi:10.1016/j.jsb.2010.05.006 Medline

68. P. B. Rosenthal, R. Henderson, Optimal determination of particle orientation, absolute hand, and contrast loss in single-particle electron cryomicroscopy. *J. Mol. Biol.* **333**, 721–745 (2003). doi:10.1016/j.jmb.2003.07.013 Medline

69. E. F. Pettersen, T. D. Goddard, C. C. Huang, G. S. Couch, D. M. Greenblatt, E. C. Meng, T. E. Ferrin, UCSF Chimera—a visualization system for exploratory research and analysis. *J. Comput. Chem.* **25**, 1605–1612 (2004). doi:10.1002/jcc.20084 Medline

70. P. Emsley, B. Lohkamp, W. G. Scott, K. Cowtan, Features and development of Coot. *Acta Crystallogr. D Biol. Crystallogr.* **66**, 486–501 (2010). doi:10.1107/S0907444910007493 Medline

71. P. D. Adams, P. V. Afonine, G. Bunkóczi, V. B. Chen, I. W. Davis, N. Echols, J. J. Headd, L. W. Hung, G. J. Kapral, R. W. Grosse-Kunstleve, A. J. McCoy, N. W. Moriarty, R. Oeffner, R. J. Read, D. C. Richardson, J. S. Richardson, T. C. Terwilliger, P. H. Zwart, PHENIX: A comprehensive Python-based system for macromolecular structure solution. *Acta Crystallogr. D Biol. Crystallogr.* **66**, 213–221 (2010). doi:10.1107/S0907444909052925 Medline

72. B. R. Bowman, M. L. Baker, F. J. Rixon, W. Chiu, F. A. Quiocho, Structure of the herpesvirus major capsid protein. *EMBO J.* **22**, 757–765 (2003). doi:10.1093/emboj/cdg086 Medline

73. X. Zhang, Z. H. Zhou, Limiting factors in atomic resolution cryo electron microscopy: No simple tricks. *J. Struct. Biol.* **175**, 253–263 (2011). doi:10.1016/j.jsb.2011.05.004 Medline

74. S. L. Ilca, A. Kotecha, X. Sun, M. M. Poranen, D. I. Stuart, J. T. Huiskonen, Localized reconstruction of subunits from electron cryomicroscopy images of macromolecular complexes. *Nat. Commun.* **6**, 8843 (2015). doi:10.1038/ncomms9843 Medline

75. S. H. Scheres, RELION: Implementation of a Bayesian approach to cryo-EM structure determination. *J. Struct. Biol.* **180**, 519–530 (2012). doi:10.1016/j.jsb.2012.09.006 Medline

76. J. F. Szilágyi, C. Cunningham, Identification and characterization of a novel non-infectious herpes simplex virus-related particle. *J. Gen. Virol.* **72**, 661–668 (1991). doi:10.1099/0022-1317-72-3-661 Medline

77. A. Kucukelbir, F. J. Sigworth, H. D. Tagare, Quantifying the local resolution of cryo-EM density maps. *Nat. Methods* **11**, 63–65 (2014). doi:10.1038/nmeth.2727 Medline